Chapter 11 – SIMULATING PILLOWING CORROSION DAMAGE

Ronald W. Gould
Structures and Materials Performance Laboratory, Institute for Aerospace Research
National Research Council Canada
Ottawa, Ontario
CANADA

11.1 INTRODUCTION

The ability to discover the accumulation of corrosion products hidden within a built-up structure is as important as being able to measure the damage so that appropriate repair and corrective actions can be determined.

Today's robotic assembly of aerospace structures tends to remove the surface deformations due to hand assembly resulting in very smooth surfaces and making the visualization of surface disturbances easier. Once located there remains the issue of determining where in the assembled layers the damage actually lies.

Hand-held eddy current devices are basic tools used to perform spot measurements to determine depth of corrosion damage. Machined blocks or sheets of the identical material are used to create calibration standards for setting up the eddy current device. The calibration standards are thus representing a machined thickness loss as corrosion damage. The issue is that the machining results in flat bottom circles or squares with straight edges which are not fully representative of real damage. When the standard consists of machined sheets assembled together into a multi-layered structure an air gap is created between the sheets at the machined sites which is also not realistic.

The simulation of corrosion pillowing will thus be divided into two parts:

1) Techniques to generate surface deformations that simulate pillowing; and
2) Those employed to artificially represent the internal damage to make the simulation sufficiently realistic.

It should be noted that to visualize the pillowing of the outer skin surface on some of the lap joint examples herein an enhanced optical technique has been employed. The D-Sight™ images were obtained through the use of a D Sight Aircraft Inspection System (DAIS) -250C (corrosion) inspection head. The DAIS are no longer available commercially but the technique remains a significant tool for visualizing subtle surface deformations characteristic of corrosion pillowing not normally detectable by un-aided close visual inspection techniques.

11.2 SURFACE DEFORMATION

Figure 11-1 shows the results of ray tracings depicting corrosion damage of increasing severity when a rivet-to-rivet and rivet row spacing ratio of 1.0 is modeled.

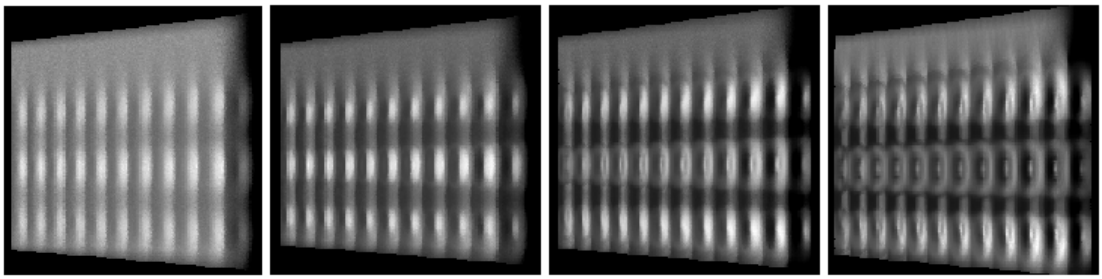

Figure 11-1: Modeling (Ray Tracings) of Corrosion Pillowing at 2, 5, 10 and 15 % Thickness Loss.

As manufacturers choose to construct joints with two or more rows of mechanical fasteners and then space them at varying intervals the characteristic deformation of these arrangements must be understood so that any simulation will be true to their response to the forces of corrosion damage. The Finite Element Models (FEM) shown in Figure 11-2 depict rivet to row spacing ratios from 1.0 to 2.0 and are accompanied by sample images of corroded joints. The rivets and rows in the Boeing 727 joint are nominally at 1.0 although the holes were drilled by hand not machine. This ratio results in the classic “pillow” with the sheet constrained at the four corners. The Lockheed L1011 joint top and middle row spacing is at 1.5 whereas the middle and bottom rows are at 1:1. This results in a “wave” when observed along the length of the joint. Both examples above are three-row joints. The McDonnell Douglas DC-9 joint is a two-row joint (the top row of rivets actually fastens separate internal “finger” doublers). The skin is very much constrained along the rivet rows and the result is that the skin must deform in a continuous wave that can only be observed when viewed perpendicular to the joint with the aid of optical means sensitive to very small displacements. It must be stated that such close rivet spacing makes the eddy current technique difficult if not impossible to apply between the rivets. Additionally, protruding head rivets can dramatically reduce the inspectable area even on a 1:1 ratio joint. Protruding head rivets also interfere with the normal practice of using grazing light to create shadows to detect pillowing as they cast the dominant shadows and limit the unobstructed viewing area.

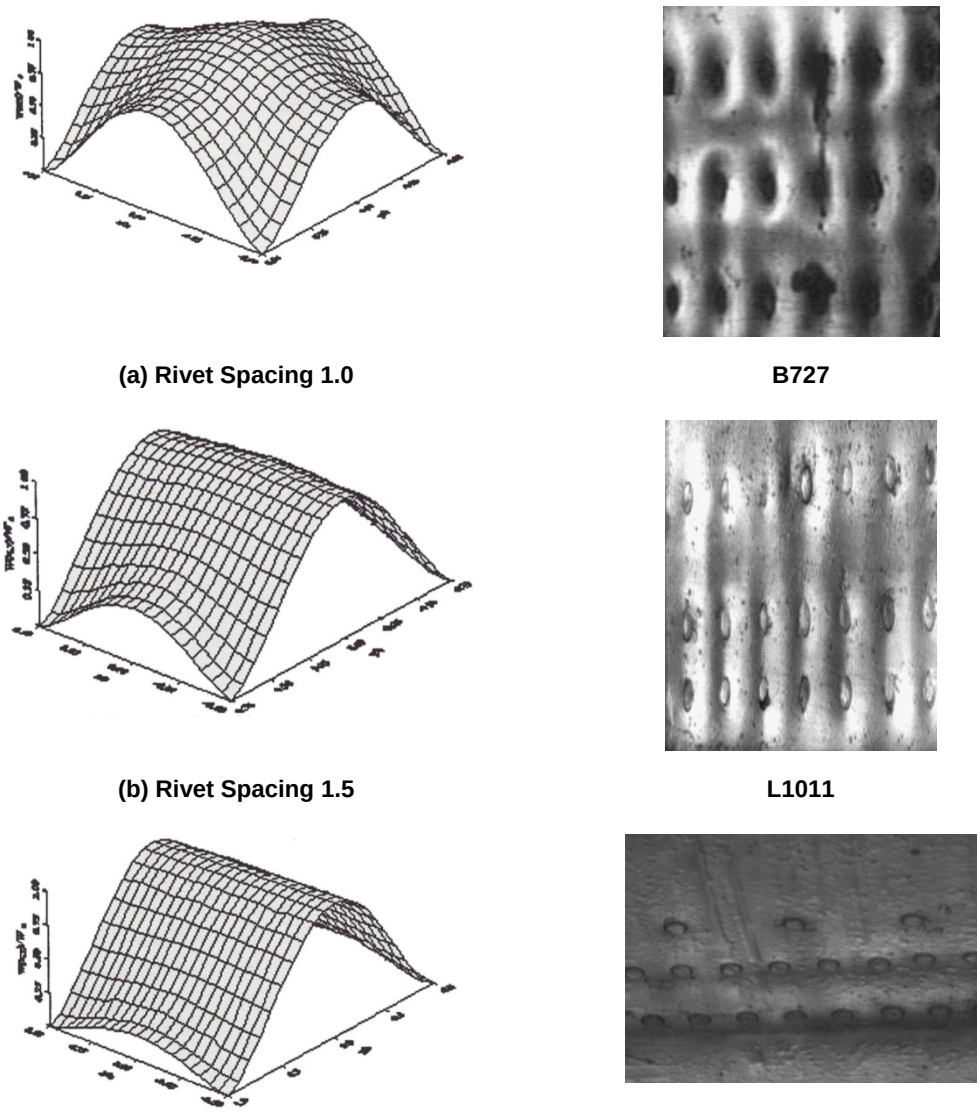

(a) Rivet Spacing 1.0 B727

(b) Rivet Spacing 1.5 L1011

(c) Rivet Spacing 2.0 DC-9

Figure 11-2: FEM Models of Varying Fastener and Row Spacings and Sample DAIS Images.

With the above considerations in mind, methods were sought to allow the surface characteristics of early corrosion damage for various lap joint constructions to be quickly simulated and studied at the smallest damage levels.

11.2.1 Mechanically Controlled Deformation

Much like the recent developments in re-configurable discrete-die tooling that controls the displacement of a field of individual pins to form sheet materials for aerospace structures, devices have been built to mechanically deform joints to simulate varying levels of faying surface damage. The intention was to be able to control the deformation between fasteners and create reference masters for optical inspection techniques. The device illustrated in Figure 11-3, Figure 11-4, Figure 11-5 and Figure 11-6 relied on two screw-driven wedges moving equally (in opposite directions) against stationary wedges attached to an internal carriage that mounted an array of hemispherically shaped pins in contact with the inner surface of the skin sheet. The sheet was riveted to the top plate of the apparatus and the pins were located at holes

through the top plate that corresponded with the centroid between the evenly spaced rivets. Small amounts of displacement could be accommodated but obtaining an even deformation across the entire array proved impossible due to bending of the carriage and sticking of the wedges. Smaller areas were successfully deformed and employed to cast dimensionally stable silicone surface replicas that themselves were used as masters for evaluating the sensitivity of enhanced optical pillowing detection devices.

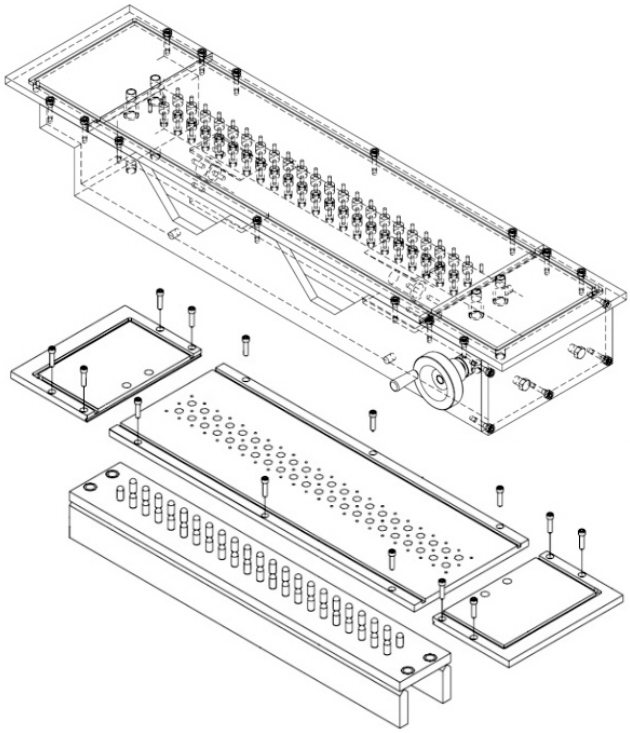

Figure 11-3: Schematic View of Dual-Ramp Pin-Pressure Pillowing Simulator.

Figure 11-4: Top View of Mechanical Pillowing Simulator.

Figure 11-5: Side View of Mechanical Pillowing Simulator.

Figure 11-6: Close-Up Side-View of Pin Contact with Underside of Skin Sheet

11.2.2 Hydraulic Pillowing

Another way of developing surface deformations to simulate corrosion pillowing is by fabricating the structure with an inflatable bladder located between the layers. Many fuselage joints are constructed with faying surface sealants or adhesive layers. The bladder was no thicker than these layers.

The bladder edges and perimeters around each fastener hole are sealed before lap joint assembly and a port is provided into the bladder. A vacuum is drawn through the port to remove all air before a liquid is introduced under pressure. Simple single-bladder lap joints were fabricated and pumped to various pressures/skin deflections using hydraulic fluid or water. To produce examples with permanent deformations at various simulated damage levels the bladder was pumped with a low temperature casting metal (i.e., Cerrobend which becomes a liquid at 70°C (158°F)) that was allowed to cool and solidify. Waxes were also liquefied, pumped and allowed to solidify.

More complex structures can also be fabricated with bladders between the skins and the stringer, tear straps, doublers and beauty strips. Therefore damage in all or only selected areas may be simulated and the external surface effects observed and recorded.

The sequence of images shown in Figure 11-10 illustrates one complete pressurization cycle for a lap joint fabricated with two 0.045 inch (1.14 mm) 2024-T3 skins and depicted in Figure 11-7, Figure 11-8 and Figure 11-9. The lap joint was hand riveted and thus not completely flat. After being deformed to a maximum fluid pressure of 80 psi (551 kilopascals) the outer surface returned to its original condition when the pressure was released.

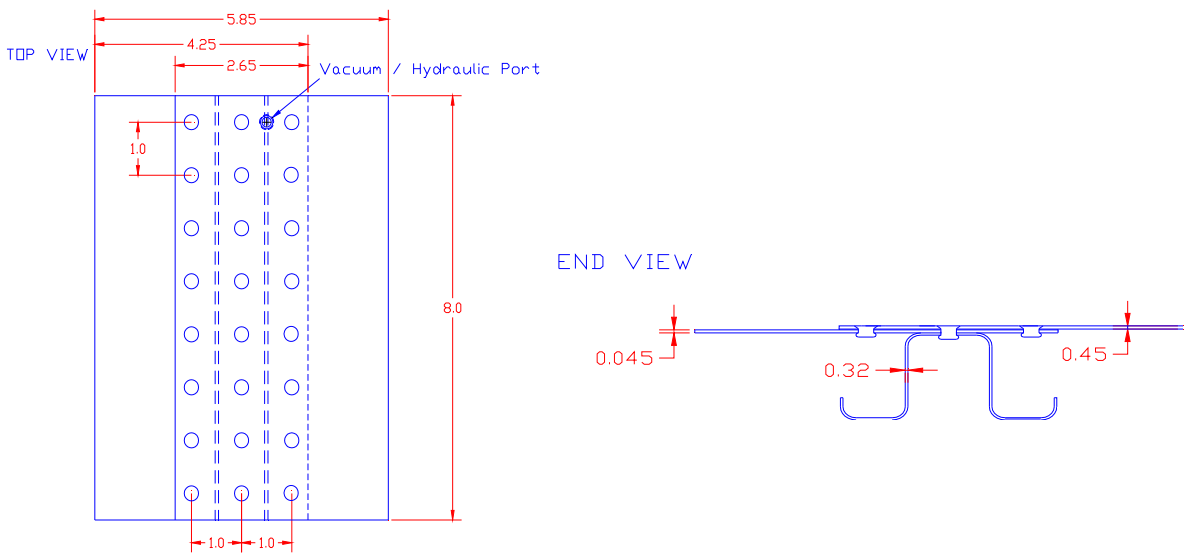

Figure 11-7: Sketch of Lap-Joint with Hydraulic Pillowing Bladder.

Figure 11-8: Overall View of Rear Surface of Hydraulic Pillowing Lap-Joint with Stringer.

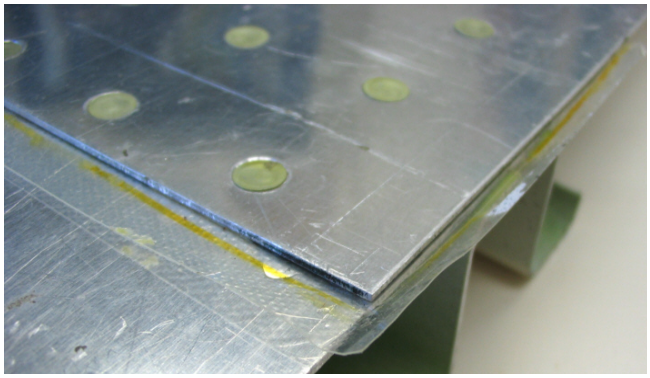

Figure 11-9(a): Close-Up of Bladder.

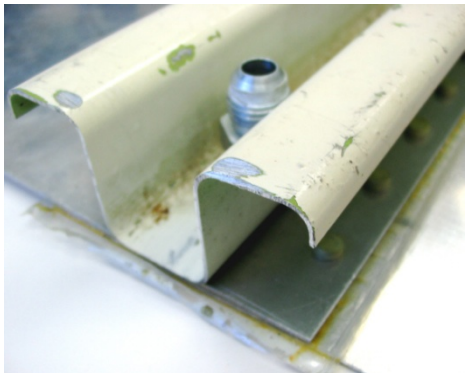

Figure 11-9(b): Close-Up of Vacuum/Hydraulic Port.

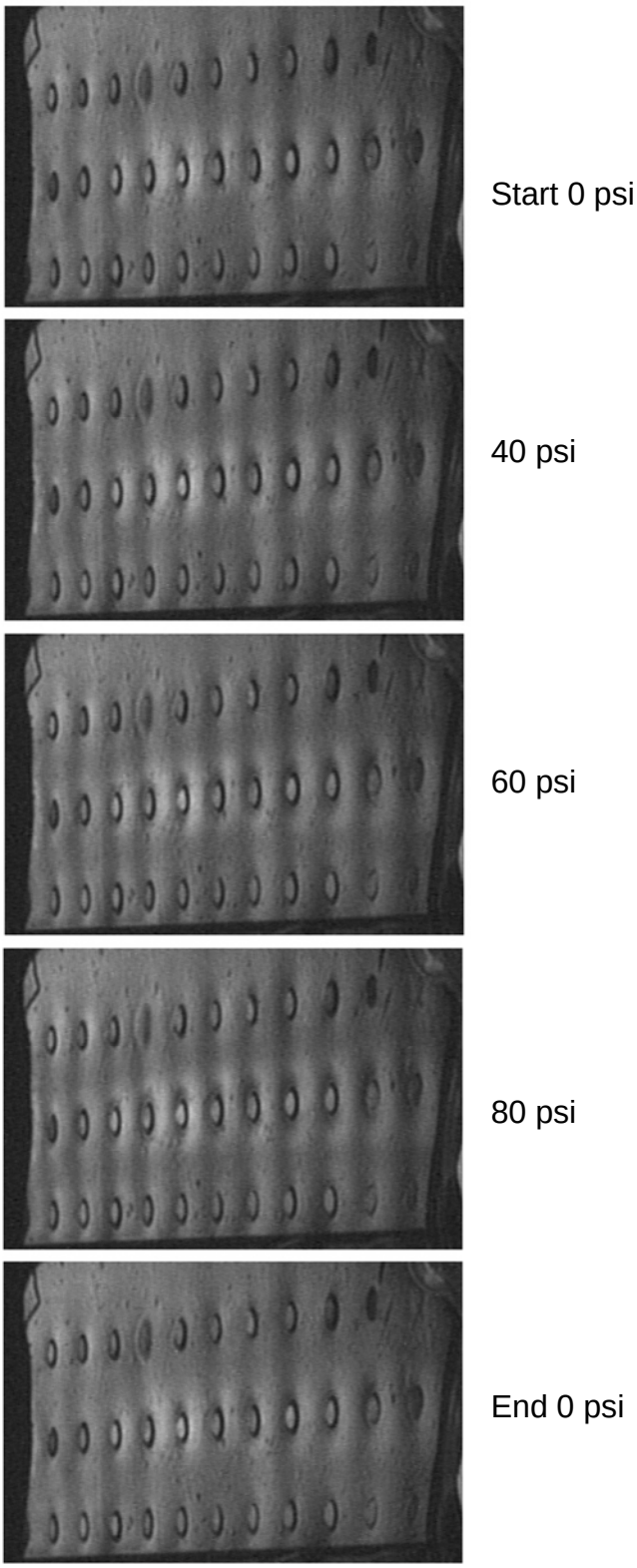

Figure 11-10: DAIS Images of One Pressure Cycle on a Hydraulic Pillowing Lap Joint.

It should be noted that the surface deformation of the hydraulic pillowing joint at 80 psi appears similar to the ray tracing model for 10% thickness loss shown in Figure 11-1.

11.3 PILLOWING DAMAGE INTERNAL SIMULATION

In-service damaged structure, if available, exhibits only the current level of corrosion pillowing. Damage formation and progression are best understood by applying artificially accelerated corrosion processes to pristine original or purpose-built new structures. The advantage of using original structure is that the alloys, protective coatings and faying surface sealants are to the manufactures exact specifications. In either case the corrosion can be monitored from the beginning. With multiple samples some can be sacrificed to teardown analysis. It is the teardown and investigation of the damage that assists in the understanding of corrosion pillowing, its simulation and its implications with respect to structural integrity.

Figure 11-11 shows a typical two-layer lap joint calibration standard with machined areas on the inner surfaces of the outer and inner skin. The circular areas were milled to specified depths to represent varying levels of corrosion damage as thickness losses. As stated in the introduction, this type of eddy current calibration standard suffers from being non-representative of the internal characteristics of the natural corrosion damage found on an aircraft. Direct comparison for damage assessment is therefore difficult.

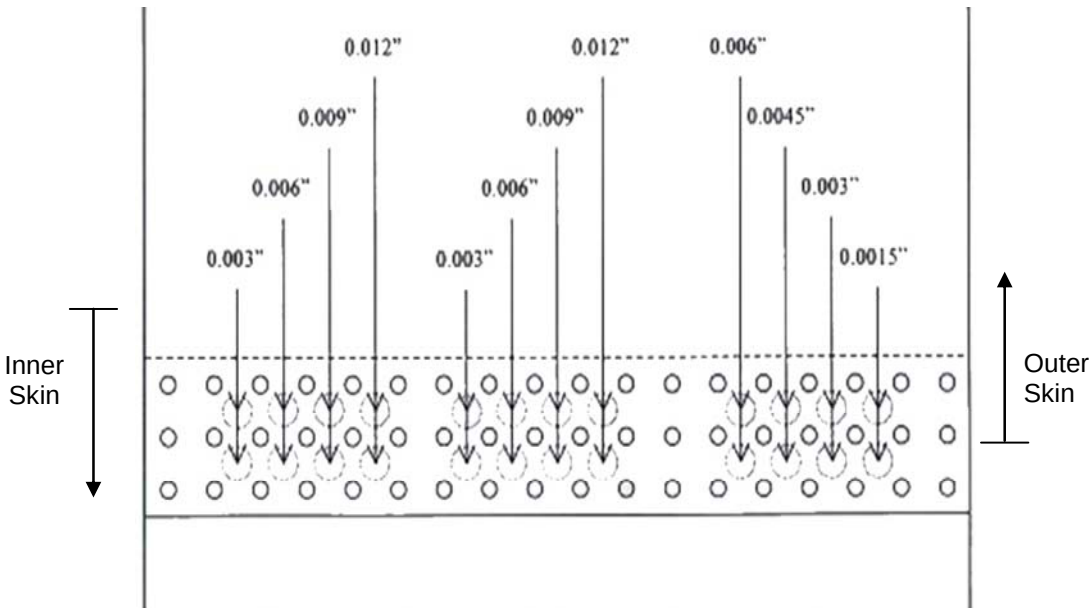

Figure 11-11: Schematic of 7075-T6 Lap Joint NDI Calibration Standard for Eddy Current with Machined Thickness Loss Simulating Crevice Corrosion Damage.

Figure 11-12 shows a robotized eddy current scan image of the entire joint area on the lap joint standard shown in Figure 11-11. A line (profile) has been taken from left to right through the area between the top and center rows of rivets. Such profiles are generated at each of four frequencies (2, 4, 7 and 12 kHz) used to scan both the standard and the suspect corroded structure. The calibration panel has machined areas of known material loss in both the front and back layers ranging from 0.0015” (0.038 mm) to a maximum of 0.012” (0.305 mm) which provide a distinctive profile related to the material loss. By comparing the deflections in the profile line from the corroded panels and from the calibration panel images it is possible to estimate the amount of material loss due to corrosion.

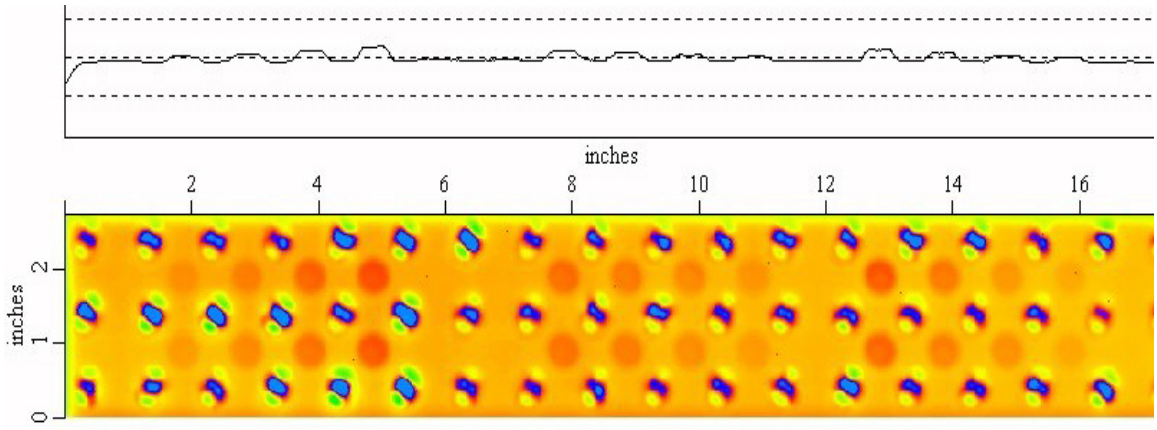

Figure 11-12: Baseline Absolute Eddy Current Scan of NDI Calibration Standard Joint at 7 kHz.

The technique described above is simple but problematic. The areas of machined thickness loss are easy to detect because they do not represent internal damage features such as corrosion product, surface topography, sealants or protective coatings. Also, the standard would not represent the external features of surface deformation or "pillowing" that result from corrosion product accumulation and volumetric increase of that product. Pillowing can cause "lift-off" difficulties with the eddy current probe contact with the surface. Figure 11-13 shows the outer surface of a lap joint undergoing accelerated corrosion where only the inner "faying" surfaces are being corroded. The outer surface is protected by a paint system. The damage is approaching 10% thickness loss yet the eddy current scan of this specimen, Figure 11-14, is not as easy to evaluate as the calibration standard.

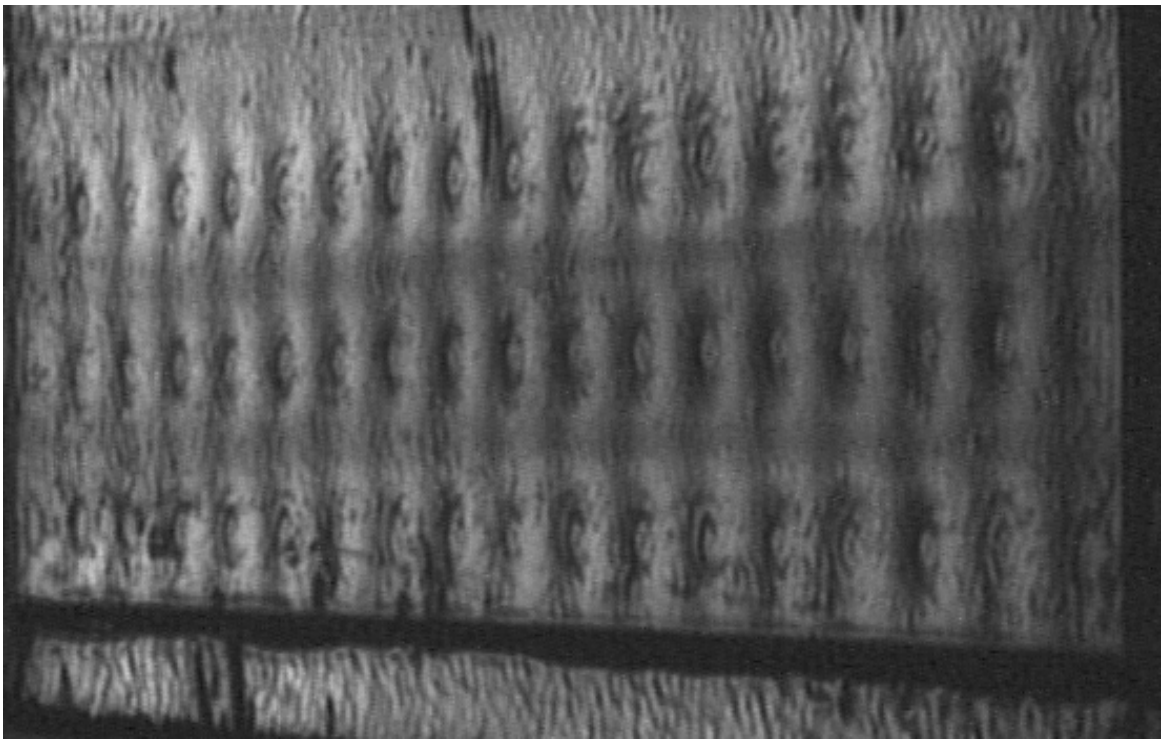

Figure 11-13: DAIS Image of Accelerated Corrosion Pillowing Following 387 Days (9288 Hours) of Salt Fog Exposure.

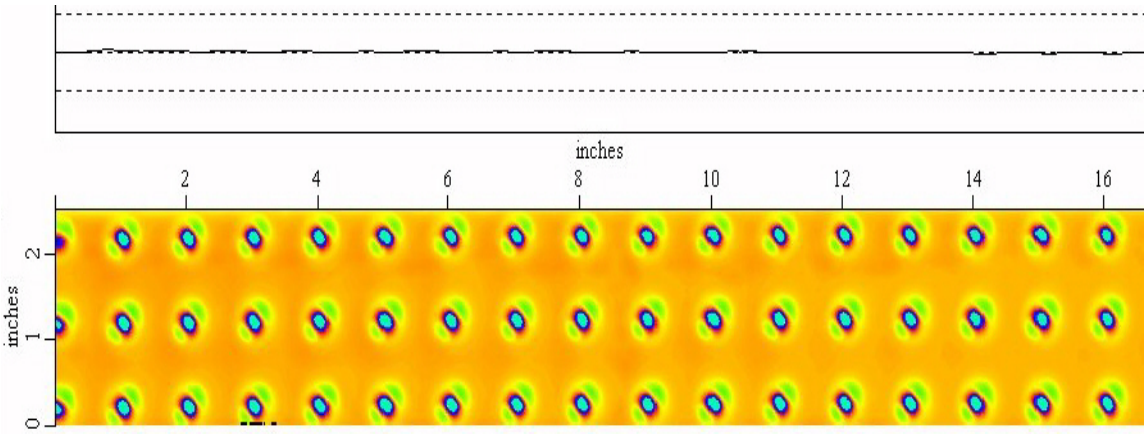

Figure 11-14: Absolute Eddy Current Scan of Accelerated Corrosion Panel at 7 kHz After 387 Days (9288 Hours) of Salt Fog Exposure to Faying Surfaces.

Note the effect of the stringer attached to the center row of rivets. This area of the outer skin is pillowed more than the upper and lower rivet rows because all the deformation (pillowing) must be outwards due to the stiffness supplied by the stringer. The inner skin at the upper and lower rivet rows can be deformed inwards and thus the outer surface deformation is less, when compared to the middle row, for the same damage level. Note also the similarity to the ray tracing model for 15% shown in Figure 11-1.

Figure 11-13 illustrates the ultimate method for simulating corrosion pillowing that being the accelerated corrosion of the subject joint design. The effort is very labour intensive and the results cannot be predicted. Protection of the surfaces that are not to be corroded is key while the specimen must be configured such that periodic inspections can be conducted to determine the presence and level of corrosion activity. Typically, months of continuous salt fog environmental conditioning are required to initiate internal damage and, as shown in Figure 11-13, more than a year was required to attain approximately 15% thickness loss damage.

11.3.1 Pillowing Measurement

Whereas the accelerated corrosion lap joint shown in Figure 11-13 shows uniform damage the simple two-layer lap shown in Figure 11-15 is more typical of natural damage found in service in that the damage is not uniform throughout. Prior to disassembly this corroded joint was measured to determine the skin deformation that upon teardown could be more directly related to the assessed internal damage.

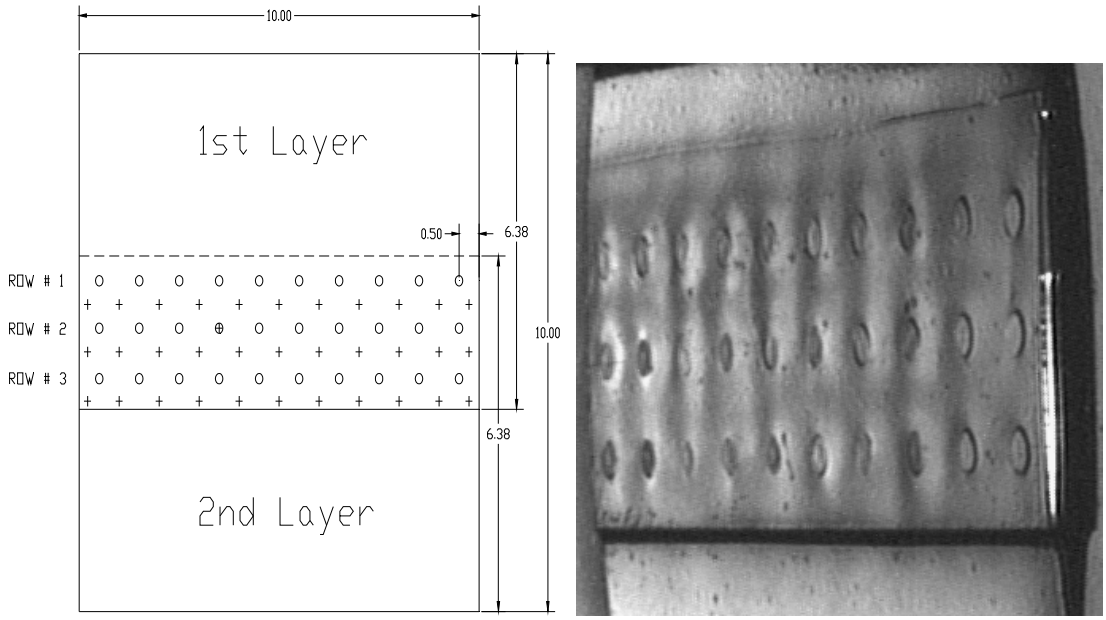

Figure 11-15: Lap Joint Panel (2024 T3, 0.040 inch, 1.016 mm Thick Skins).

The table of measurements below is in two parts. The measurements were taken with a deep throat micrometer and three measures were averaged for each result. The top group of measurements is of the total thickness measured at the locations shown in the drawing above, for the three rows. The bottom group of measurements is the pillowing (theoretical pristine lap thickness deducted from values in top table).

Table 11-1: Pillowing Measurements of the Two-Layer Lap Joint Shown in Figure 11-15.

						1st Layer	**0.040**				
	1	**2**	**3**	**4**	**5**	**6**	**7**	**8**	**9**	**10**	**11**
a	0.108	0.097	0.098	0.096	0.104	0.095	0.096	0.095	0.094	0.089	0.092
b	0.096	0.097	0.096	0.092	0.095	0.093	0.094	0.098	0.099	0.092	0.091
c	0.092	0.096	0.094	0.092	0.093	0.100	0.097	0.105	0.095	0.091	0.092
						2nd Layer	**0.040**			**Zero**	**0.001**

	1	**2**	**3**	**4**	**5**	**6**	**7**	**8**	**9**	**10**	**11**
a	0.027	0.016	0.017	0.015	0.023	0.014	0.015	0.014	0.013	0.008	0.011
b	0.015	0.016	0.015	0.011	0.014	0.012	0.013	0.017	0.018	0.011	0.010
c	0.011	0.015	0.013	0.011	0.012	0.019	0.016	0.024	0.014	0.010	0.011

11.3.2 Machined Simulation

Careful teardown and corrosion product removal was applied to both natural and artificially corroded structures to enable the interrogation of the damaged area. The exposed corrosion product was removed by use of a chemical process to avoid further mechanically induced abrasive damage. The chemical cleaning process permitted a better appreciation for the surface topography on the remaining metal. The teardown and cleaning also pointed to the fact that the clamp-up provided by the rivets means that the last locations to suffer corrosion damage within the joint are those nearest the fasteners.

The objection to the flat-bottomed machined thickness loss areas used on the typical calibration standard (Figure 11-11) was first addressed by creating an Electric Discharge Machining (EDM) tool electrode that incorporated a rough face. When this rough-faced tool was worked to the desired depth the result would be a surface topography emulating the surface condition previously observed on the cleaned corroded specimens. A calibration standard prepared in this way would thus be more realistic [1].

The inner surface of a CNC machined sheet shown in Figure 11-16 incorporates the observations and thickness loss values from disassembled and cleaned corroded lap joint skins. The maximum thickness loss is in the zone between the fasteners and tapers towards the edges and fastener locations. The as-machined condition for various thickness loss or damage levels is shown in Figure 11-17. The CNC machined surfaces were then hand sculpted to give them unique surface topographies. These coarsely roughened areas were then lightly sandblasted to better represent corrosion surface damage, Figure 11-18. This technique is an improvement on the EDM method since the topographies are unique.

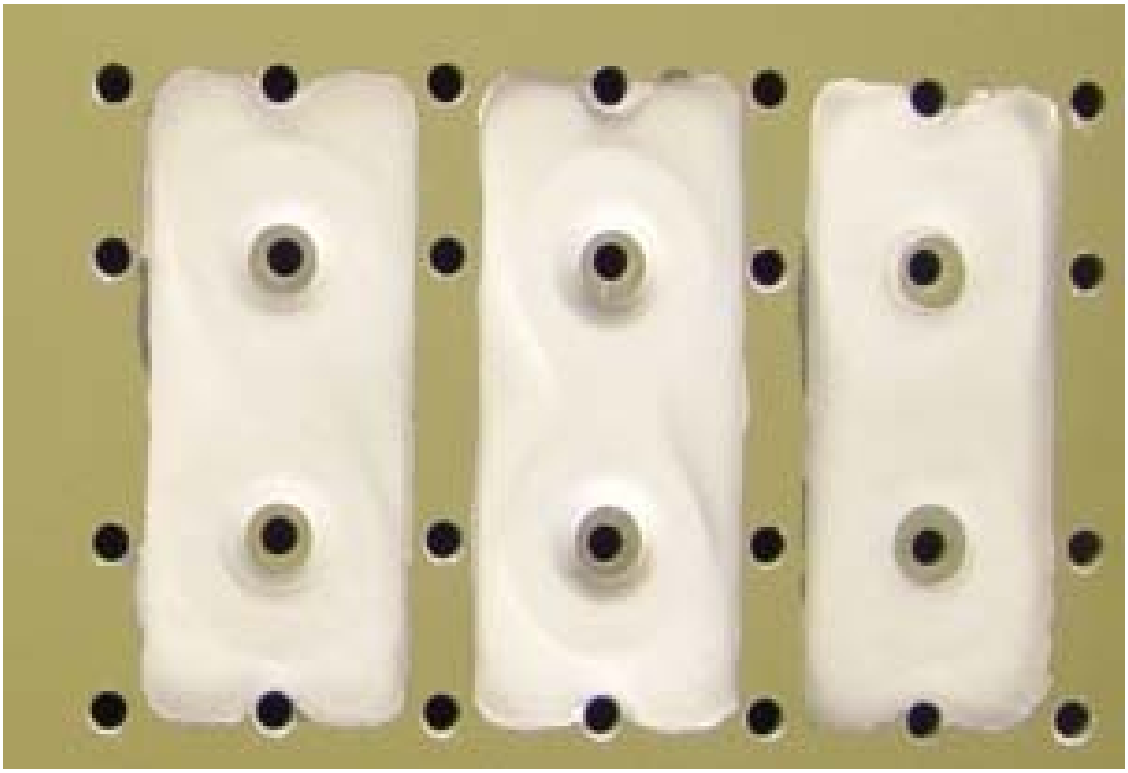

Figure 11-16: Faying Surface of One 2024-T3 Skin for a Simulation of Crevice Corrosion and Pillowing.

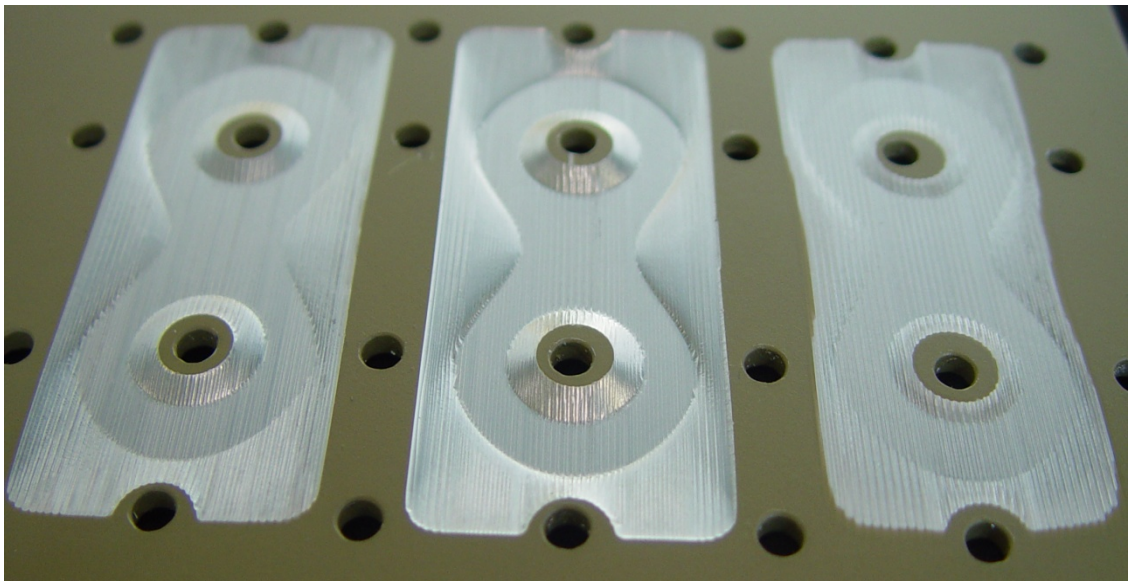

Figure 11-17: CNC Machined Corrosion Damage Thickness Loss to Three Depths (30, 50 and 10 %).

Figure 11-18(a): Machined Areas Hand-Ground.

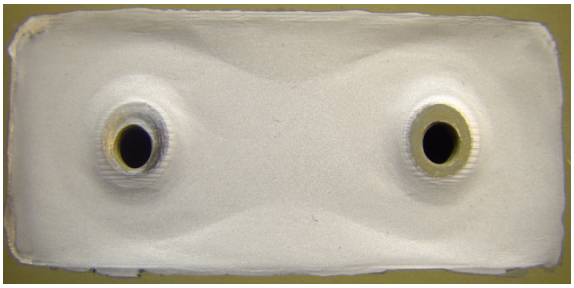

Figure 11-18(b): Surface Sandblasted.

The sandblasted surface offers more natural exposure to the aluminum grains and grain boundaries in comparison to the surface following the milling and grinding. Without sandblasting the corrosive attack would be more likely to advance along the small scratches remaining from the machining.

The machined and artfully sculpted surfaces were then subjected to a short period of accelerated corrosion. Although attack by both ANCIT and EXCO solutions was tried the best results were achieved through exposure to Copper Assisted Salt Fog (CASS).

Once the “corroded” areas were individually prepared the voids were packed with aluminium oxide to the volume required by the thickness loss and the calibration standard was assembled by attaching the inner sheet which was not machined. Assembly with the corrosion product *in situ* proved very difficult especially in the proper formation of the shop head of the rivets. Special tooling was devised to deform and squeeze the skins together so that successful riveting could be achieved. The loose aluminium oxide powder also posed a problem as it shifted during assembly. Figure 11-19 shows the assembled joint. Figure 11-20 shows a later more successful pillowing simulation joint.

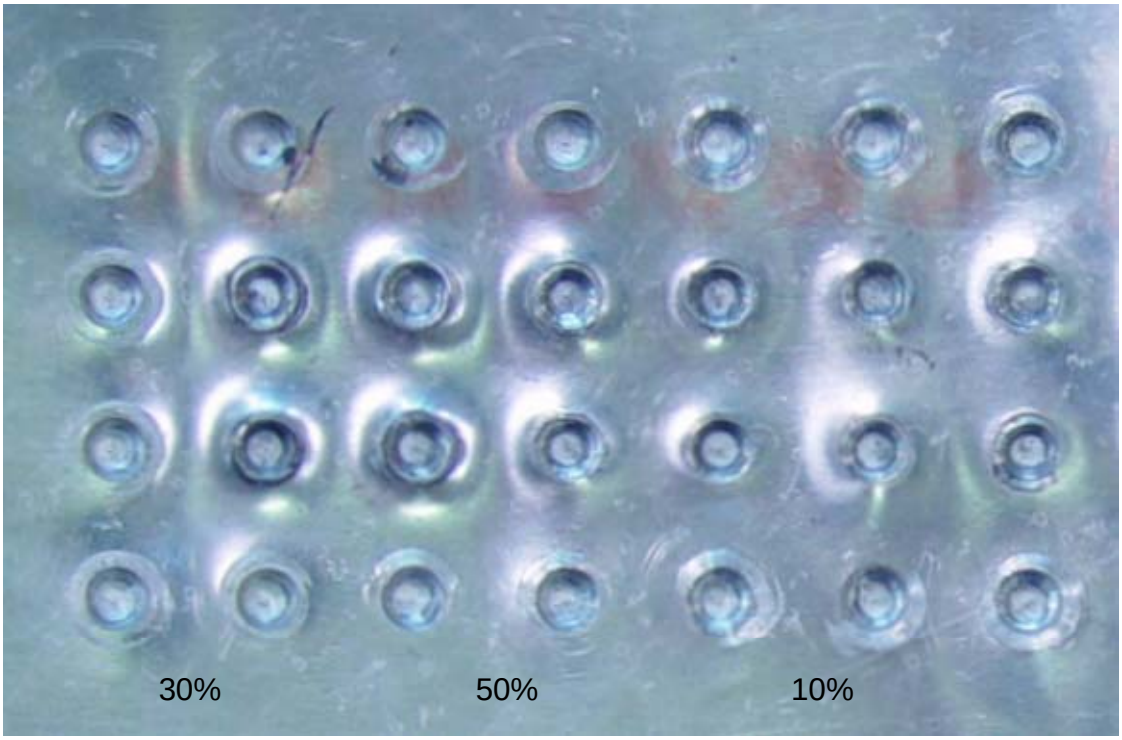

Figure 11-19: Assembled Joint.

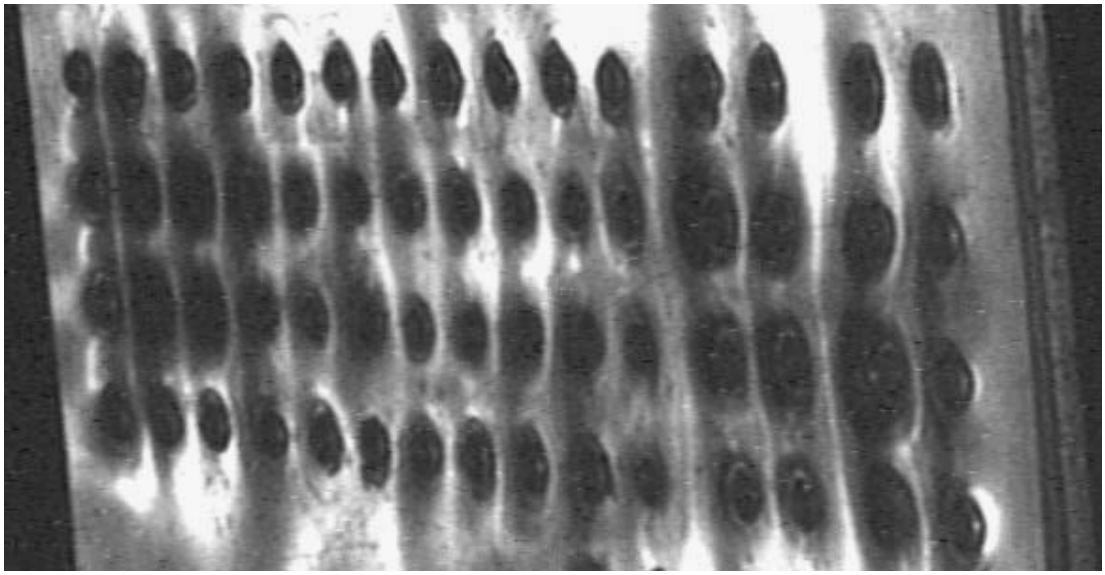

Figure 11-20: DAIS Image of Machined Simulation Panel with Corrosion Product Included.

11.3.3 Pillowing Cracks

One of the insidious effects of corrosion pillowing is the development of non-surface-breaking, high aspect ratio cracks originating on the faying surfaces (inner surfaces and thus not visually detectable). Whereas fatigue cracks may originate from fastener holes and run longitudinally due to hoop stresses under cyclic pressurization, these “pillowing cracks” are driven by tensile forces, originate away from the

fastener holes and they can grow in any direction. To date this feature has not been simulated in a lap joint calibration standard but the phenomenon has been demonstrated in an accelerated corrosion process.

The lap joint illustrated in Figure 11-21 was assembled with one aluminium and one clear acrylic skin. The two skins were assembled with screws not rivets and the assembly was exposed to a corrosive environment. The acrylic skin panel was intended to facilitate visualizing and documenting the damage onset and progress of the accelerated corrosion process.

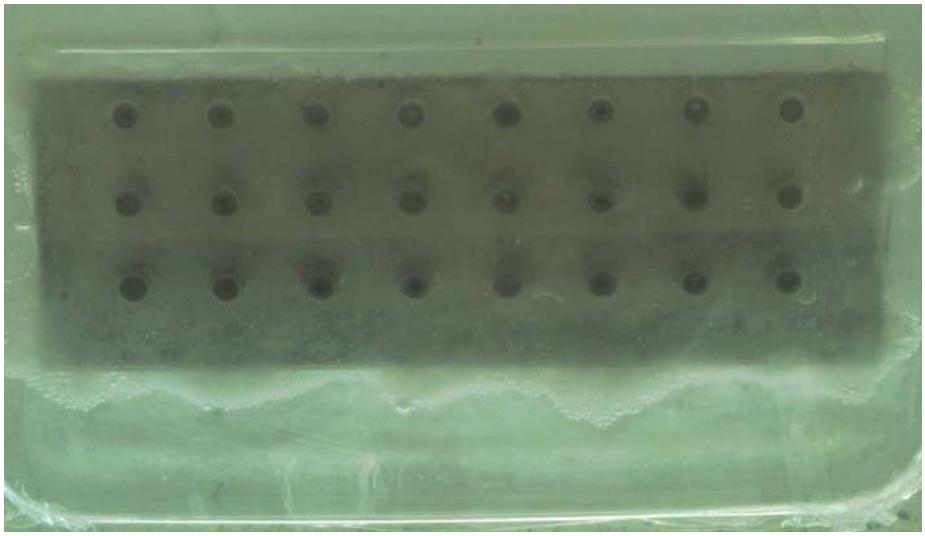

Figure 11-21: Al/acrylic Hybrid Lap Joint After 15 Days Exposure to EXCO Solution.

Figure 11-22 shows the outer surface of the aluminium skin before and after exposure to the corrosive environment. Unexpectedly this set-up helped in recognizing the formation of pillowing induced cracks, as shown in Figure 11-23.

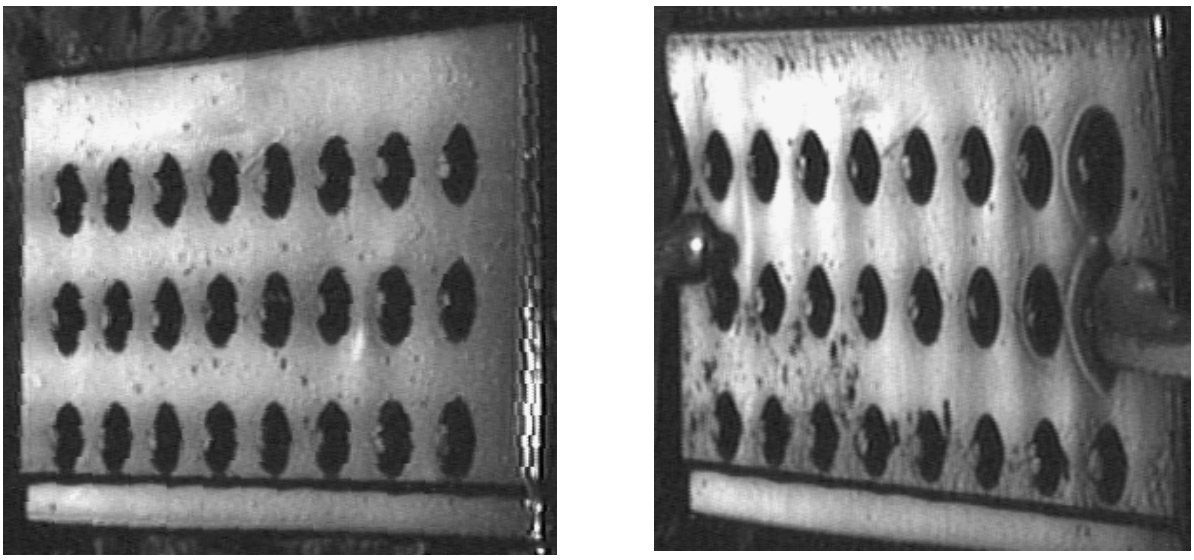

(a) **(b)**

Figure 11-22: DAIS Images of Aluminum Outer Skin Front Surface: (a) Before; and (b) After Corrosion.

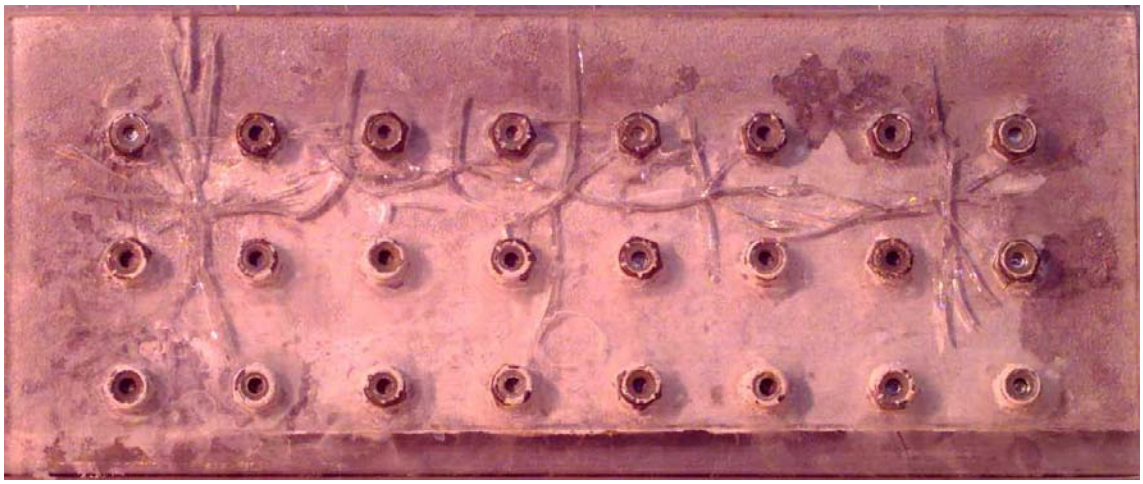

Figure 11-23: Cracks in Acrylic Inner Skin Caused by the Force of Corrosion Product Accumulation.

11.3.4 Wing Plank Simulated Corrosion Damage Calibration Standard

The lessons learned in modelling and teardown used to facilitate the fabrication of fuselage lap joint pillowing calibration standards were applied to thicker plate material to provide standards for general, spot and pitting corrosion in the machined step joint on wing skin material (7075-T6). Figure 11-24 shows the two adjacent 87-inch (221 cm) long wing planks. A sketch of the three locations for the various damage sites is shown in Figure 11-25. The Bottom Of Top (BOT) and Top Of Bottom (TOB) sites were assembled with the mandated sealant applied once the damage had been introduced. The Bottom Of Bottom (BOB) sites were unique in that the inserted corrosion product had to remain in place and this was achieved by using an adhesive.

Figure 11-24: Wing Planks.

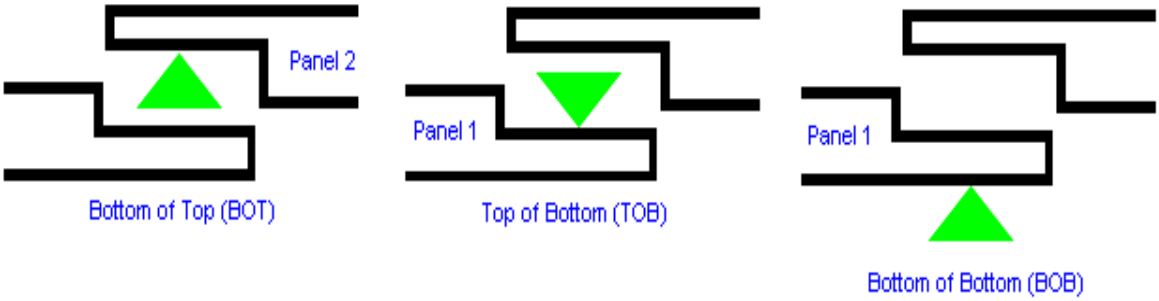

Figure 11-25: Location of Damage Sites.

The thickness of each plank was measured adjacent to each damage site and these local measurements were used to determine the amount of material to be removed. For "area" corrosion damage sites a 0.375 inch (9.5 mm) diameter end mill was used to remove material down to within a few thousands of an inch from the final desired dimension. This small thickness was left so that the surface could include some gross topographical roughness without exceeding the desired mean thickness. Blending from the flat bottom of the milled site to the level of the surrounding undamaged surface was done by hand with a Dremel tool and high speed steel bits. Artificial corrosion of the surface was induced to provide the micro-roughness associated with natural corrosion damage and the period of exposure was controlled to match the severity of the thickness loss (Figure 11-26).

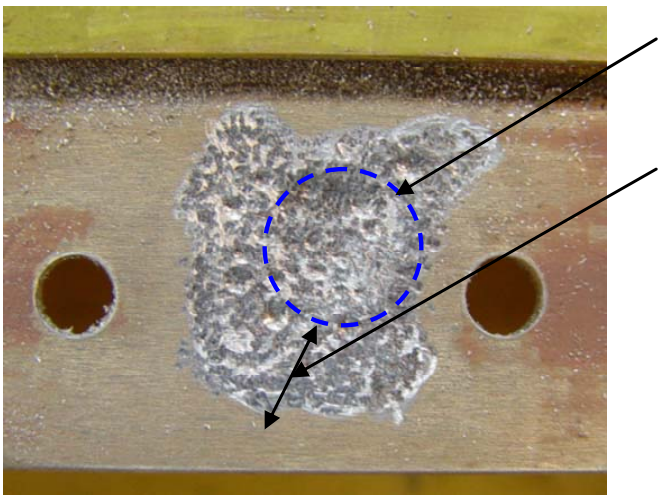

Area flat-bottom end milled to near full depth.

"Artistic" blend-out to full thickness.

Note also "Artistic" macro surface roughness features and less blending towards fasteners in appreciation of less damage due to clamp-up.

Figure 11-26: Typical "Area" Damage Site Preparation Prior to Corrosion Solution Application.

Smaller features were included such as minor Surface Corrosion (SCOS) and corrosion pits (Figure 11-27). Only the area and surface corrosion sites were back-filled with corrosion product. In this case the corrosion product used was harvested from naturally occurring corrosion of identical material.

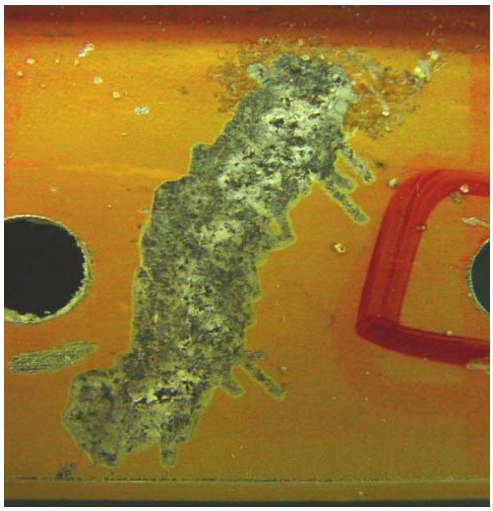

Figure 11-27(a): Corroded SCOS Damage Site.

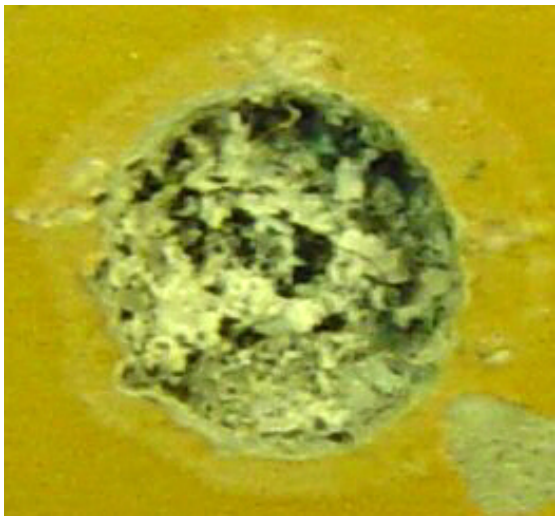

Figure 11-27(b): Corroded Pit.

The "SCOS" damage was machined entirely by hand and the depth measured by a dial gauge with a needle nose attachment. The "Pit" damage sites were counter-bored by hand and the depth measured by dial gauge.

As described above, the lessons earned in developing lap joint pillowing and corrosion simulation calibration masters has permitted the simulation of similar damage in wing plank joints.

As a complimentary development to the wing plank corrosion joint, a wing plank joint was prepared with induced cracks to challenge the current tools and techniques used to detect them. With special tooling, forced overload cracks could be inserted at any fastener hole, run in any direction and the length of the crack could be controlled. Ultimately both simulated corrosion and crack damage could be combined in one wing plank joint.

11.4 CONCLUSIONS

It has been demonstrated that corrosion occurring between the faying surfaces of aluminum aircraft structures introduces damaging stresses. These stresses are due in part to the loss of thickness of the structural skins and to the accumulation of high volume corrosion products between the skins. Both contribute to plastic deformation and cracking of the skins. This plastic deformation has been referred to as pillowing and it is usually most pronounced in the outer layer of skin where it is seen as an undulating surface profile. The amplitude of the undulations is a direct indication of the severity of corrosion and of the loss of thickness of the associated metal sheets. However, quantitative measurement of thickness loss requires that carefully prepared calibration standards be available. A number of methods have been developed to produce the standards and perform these calibrations, employing either optical or electro-magnetic methods. These methods have been described and their merits and limitations have been explained. Of particular concern is that pillowing induced cracking often occurs on the inside surfaces of the skins and is therefore not seen during direct visual examination. This makes the assessment of corrosion severity of particular importance, and thus reinforces the need for accurate calibration of the available detection methods. It is also important to be able to simulate the corrosion that occurs in service in a well controlled laboratory environment.

11.5 REFERENCES

[1] Chapman, C.E., National Research Council Canada, Private Communication.